# Extraction of nuclear level densities from neutron spectra emitted in proton-induced reactions on lead isotopes and Bi

A. Wallner, B. Strohmaier, and H. Vonach
*Institut für Radiumforschung und Kernphysik der Universität Wien, Boltzmanngasse 3, A-1090 Vienna, Austria*
(Received 5 July 1994)

Neutron-production spectra from $(p,n)$ reactions on $^{204,206,207,208}$Pb and $^{209}$Bi measured previously by a Russian group were analyzed to extract numerical values for the level densities of the residual nuclei up to excitation energies of 5–6 MeV with uncertainties of 20–50%. Comparisons with the Gilbert-Cameron form and various parametrizations of the Ignatyuk formulation indicate that the Ignatyuk model with original parameters describes the results well whereas the other forms yield lower level densities. The agreement with the results of the first analysis by the experimenters themselves varies over the range of nuclei considered, being poorest for $^{204,206}$Bi.

PACS number(s): 21.10.Ma, 24.60.Dr, 25.40.Kv, 27.80.+w

## I. INTRODUCTION

The purpose of this investigation is to determine the level densities of the residual nuclei of $(p,n)$ reactions on $^{204,206,207,208}$Pb and $^{209}$Bi. To this end, neutron-production cross sections differential with respect to energy were analyzed in the frame of nuclear-reaction models. The underlying experimental data which were all measured at the Institute for Physics and Power Engineering, Obninsk, Russia, existed at 11.2 MeV and — for some of the nuclides — at 6.95 MeV incident proton energy.

The interest in nuclear level densities comes from the fact that for nuclear-reaction model calculations the consideration of residual states is necessary, which can be realized by the individual characteristics of each level only in a very limited energy range. At increasing excitation energies, one has to rely on a statistical description of the properties of the nuclei, i.e., use level-density formulas. Starting from the Fermi-gas model, over the past decades various phenomenological models of increasing refinement were developed, with the goal to also enable the inclusion of effects of shell closure, pairing, and collective degrees of freedom. Studies such as the present are required for the validation of such phenomenological formulations of the level density as well as of the systematics which are often used for their model parameters to provide input data for routine calculations of nuclear-reaction cross sections.

The item of nuclear level densities was considered as sufficiently important by the International Atomic Energy Agency to install a Coordinated Research Programme (CRP) dedicated to the measurement of neutron-emission spectra in reactions induced by protons and alpha particles and their analysis with regard to nuclear level densities [1]. Following the IAEA's guidelines for such CRP's, like experiments were to be performed by various of the participating laboratories in order to have a cross-check of the experimental and theoretical results. The duration of this particular CRP was from 1986 to 1989, and the data under investigation here were measured and first analyzed in the framework of this CRP. The present work is a later contribution to this CRP with the additional objective to achieve an estimate of the uncertainties of the deduced level densities by ways of parameter variations in the model calculations as well as by consideration of all uncertainties of the analyzed experimental data.

In Sec. II, a short summary of the method applied is given; in Sec. III the experimental data used for the analysis are discussed in more detail. Section IV contains a description of the computer codes used and their model options. In Sec. V, we describe the choice of parameters and discuss our results.

## II. METHOD

The procedure used here was proposed [2] at the IAEA Advisory Group Meeting on Basic and Applied Problems of Nuclear Level Densities and was applied in the framework of the IAEA Coordinated Research Program on Measurement and Analysis of Double-Differential Neutron-Emission Spectra in $(p,n)$ and $(\alpha,n)$ Reactions. The method relies on the fact that the nuclear level density is one of the most crucial ingredients of statistical model calculations. The analysis of compound-nucleus reactions by means of Hauser-Feshbach calculations may, therefore, serve for extracting level densities.

The cross section for population of a level $(E_k, I_k, P_k)$ of the residual nucleus by emission of a particle of type $b$ from a compound system formed by absorption of particle $a$ is given by

$$\sigma_b(\varepsilon_a,\varepsilon_b)=\sum_{J\Pi}\sigma_a^{\mathrm{CN}}(\varepsilon_a)\frac{\Gamma_b(U,J,\Pi,E_k,I_k,P_k)}{\Gamma(U,J,\Pi)}\ , \quad (1)$$

where $U$, $J$, and $\Pi$ are the energy, angular momentum, and parity of the compound nucleus, $E_k$, $I_k$, and $P_k$ the energy, angular momentum, and parity of the residual nucleus, $\varepsilon_a$ and $\varepsilon_b$ the energies of relative motion for incoming and outgoing channels ($\varepsilon_b = U - E_k - B_b$

 

where $B_b$ is the separation energy of particle $b$ from the compound nucleus), $\sigma_a^{\rm CN}$ is the cross section for formation of a compound nucleus with spin $J$ and parity $\Pi$, $\Gamma_b(U,J,\Pi,E_k,I_k,P_k)$ is the decay width of the compound nucleus to level $(E_k,I_k,P_k)$ of the residual nucleus by emission of particle $b$, and $\Gamma(U,J,\Pi)$ is the total decay width of the compound nucleus, which includes all possible decay modes that are consistent with the conservation laws, and contains the residual states of all particle channels $b'$ as functions of residual-nucleus excitation energies $E'$. Analogously, the energy-differential particle-emission cross section for population of continuum states is

$$\frac{d\sigma}{d\varepsilon_b}(\varepsilon_a,\varepsilon_b) = \sum_{J\Pi}\sigma_a^{\rm CN}(\varepsilon_a)\frac{\sum_{IP}\Gamma_b(U,J,\Pi,E,I,P)\rho_b(E,I,P)}{\Gamma(U,J,\Pi)} \quad (2)$$

with

$$\Gamma(U,J,\Pi) = \sum_{b'}\left(\sum_{I'P'}\int_{E_c}^{U-B_{b'}} dE'\Gamma_{b'}(U,J,\Pi,E',I',P') \times\rho_{b'}(E',I',P') + \sum_k \Gamma_{b'}(U,J,\Pi,E_k,I_k,P_k)\right) . \quad (3)$$

Here, the $k$ summation is over the discrete levels in channel $b'$ and $E_c$ is the continuum edge in this channel.

If $b$ represents the majority channel, as neutron emission does in proton-induced reactions on heavy nuclei, then it is evident that a good description of those regions of the emission spectrum leading to continuum states can be achieved even though $\rho_b(E,I,P)$ may be wrong by a factor: since $\Gamma$ is essentially determined by the decay width of that same channel, this factor will cancel. If, however, simultaneous description of the cross section in a minority channel is demanded, preferably of the population of states which are described individually and not by a level density, then no such cancellation can occur, since in the numerator no level density enters, and $\Gamma(U,J,\Pi)$ can be determined correctly.

In order to extract the level density of a residual nucleus, we proceed in two steps.

(a) A suitable formulation of the energy dependence of the total level density is chosen and the parameters adjusted such that the cross section calculated by means of Eq. (1) fits the measured value, i.e., the reproduction of the spectrum in the energy region of discrete levels ("minority channel") is claimed. In this way, the total width is determined.

(b) Using this total level density, we simultaneously calculate the cross section for the continuum states $d\sigma/d\varepsilon_b$ [Eq. (2)]. The level density can be further improved by binwise renormalization of the ratio of calculated to experimental differential cross section in the continuum energy region ("majority channel"):

$$\rho_b(E,I,P) = \rho_b(E,I,P)|_{\rm assumed}\frac{d\sigma/d\varepsilon_b\big|_{\rm meas}}{d\sigma/d\varepsilon_b\big|_{\rm calc}} . \quad (4)$$

This equation holds on the presupposition that there is equality of measured and calculated cross sections for population of the discrete levels used for the determination of the Hauser-Feshbach denominator, and that deviations between theory and experiment in the continuum region of the spectrum are entirely due to deficiencies in the level-density description. The influence of other quantities is discussed in connection with the uncertainty estimate in Sec. V. Also, Eq. (4) relies on the assumption that the renormalization of the level density does not spoil the reproduction of the cross section in the discrete-level region. This requires that the description of the experimental data by the theory must be already rather accurate, so that the renormalization factors of Eq. (4) remain close to unity. Otherwise, the renormalization would lead to a substantial change of the Hauser-Feshbach denominator, if—as in our case—the reaction considered gives a large contribution to the total width $\Gamma$ [Eq. (3)]. If the level-density determination [step (b)] is done for a minority channel like $\alpha$-particle emission, correct level densities can be derived to a large extent independently of the quality of the level-density assumptions in the calculations. For the analysis of neutron emission, however, which represents most of the total reaction cross section for medium-mass and heavy nuclei, a good initial choice of the level density for the analysis remains essential. On one hand, this complicates the analysis, but on the other—if the conditions can be met—it provides an additional consistency check supporting the validity of the method used.

So far, only a compound-nucleus reaction mechanism has been considered. In fact, there is a contribution of preequilibrium reactions which increases with increasing incident proton energy. Still, the method may work reasonably well if the amount and energy dependence of the preequilibrium contributions in both steps (determination of $\Gamma$ and description of the spectra in continuum bins) are described sufficiently accurately. For the calculation of the renormalization factors [Eq. (4)], it is necessary to calculate the noncompound cross sections theoretically and subtract them from the experimental neutron-emission cross sections, before the latter are divided by the corresponding quantities calculated in the compound-nucleus model. For reactions with different particles in the entrance and exit channels and relatively low bombarding energies, it is justified to neglect direct reactions and restrict the correction to contributions from preequilibrium processes.

## III. UNDERLYING EXPERIMENTAL DATA

The present work is a reanalysis of the experimental data measured and first interpreted by Zhuravlev *et al.* [3] and Biryukov *et al.* [4].

Neutron-production spectra of proton-induced reactions exist for incident energies of 6.95 and 11.2 MeV for $^{207,208}$Pb$(p,n)$ and $^{209}$Bi$(p,n)$, and for 11.2 MeV only for $^{204,206}$Pb$(p,n)$. The lower incident energy offers the advantage that preequilibrium effects are clearly negligible. The targets consisted of metal foils of about 20 mg/cm$^2$ areal mass density, which leads to a maximum energy loss of the incident protons of about 0.4 MeV. The neutron-emission cross sections were determined by the time-of-flight method using a flight path of 2.5 m and a time resolution of 3.5 ns, resulting in an energy resolution of $\approx$ 0.75 MeV at 7 MeV, the upper end of the neutron spectra. The angle-integrated neutron-emission cross sections were derived from the double-differential ones, measured at four angles at least, with the exception of the 6.95-MeV measurements on $^{207,208}$Pb where only one measurement was performed, namely at $\theta = 105°$. At this low incident energy, neutron emission, however, is known to be isotropic and can thus be calculated from measurements at one angle. The finite resolution both in the incident proton energy and the measured neutron energy was accounted for by averaging calculations for two incident energies (10.9 and 11.1 MeV and 6.6 and 6.8 MeV, respectively,) and folding the calculated neutron spectra with a Gaussian resolution function with an energy-dependent width equal to the experimental energy resolution.

## IV. COMPUTER CODES AND MODEL OPTIONS

The model calculations were performed with the code GNASH [5]. It utilizes the Hauser-Feshbach statistical model, together with the exciton model for preequilibrium decay, assuming that the reaction proceeds as a series of binary reaction stages. Width fluctuations can be applied, for which the correction factors have to be provided externally. Minor changes of the program GNASH [5] were necessary for the special case considered here, namely, for incident protons.

The Hauser-Feshbach formula is given in Eqs. (1) and (2) for population of discrete levels and continuum-energy bins, respectively. The reaction cross section for formation of the compound nucleus $\sigma_a^{\rm CN}$ can be expressed in terms of the optical model transmission coefficients $T_l^a(\varepsilon_a)$; $\Gamma_b$, the decay width of the compound nucleus into the state $(E,I,P)$, and the total width $\Gamma(U,J,\Pi)$ [Eq. (3)] can be related to the transmission coefficients $T_l^b(\varepsilon)$ and to the level densities of the appropriate nuclei. All transmission coefficients are input to GNASH via an external file.

In order to generate these transmission coefficients, the nonrelativistic code SCAT2 by Bersillon [6] was used. This program calculates the total, the shape-elastic, and the total reaction cross section, as well as the transmission coefficients as functions of energy and orbital angular momentum within the phenomenological optical model.

For protons, five different optical potentials were investigated. Proton-induced reactions on heavy elements proceed nearly completely via neutron emission. Therefore the calculated total reaction cross section can be compared with the measured total neutron-emission cross section. The reproduction of this cross section at proton energies of 6.95 and 11.2 MeV was the only criterion for the choice of a proton optical potential; its continuation to other energy regions does not play a role since protons in outgoing channels do not. The potentials of Perey [7], Mo and Davis [8] and of Mani, Melkanoff, and Iori [9] deliver cross sections that are about 30–40 % lower than the value measured for 11.2 MeV incident protons on $^{208}$Pb. On the other hand, the global potential of Becchetti and Greenlees [10] and that of Mahaux and Sartor [11] determined for $^{208}$Pb show very good agreement with the emission cross sections. The potential of Becchetti and Greenlees [10] was used further in the calculations.

For a proper description of the emission spectra, a good choice of the neutron transmission coefficients in the energy range up to 7 MeV was necessary. To achieve this, a reasonable reproduction of the total and the nonelastic cross section in this range was aimed at. Several potentials were investigated: the global ones of Becchetti and Greenlees [10], Wilmore and Hodgson [12], Engelbrecht and Fiedeldey [13], and of Rapaport, Kulkarni, and Finlay [14], as well as the potentials of Lawson, Guenther, and Smith [15], Finlay *et al.* [16], and Mahaux and Sartor [17] determined for this particular mass range. In Fig. 1, the nonelastic cross sections calculated with these potentials for $^{\rm nat}$Pb are displayed. At low neutron energies, a width-fluctuation correction was applied, with the correction factors calculated with the statistical model code STAPRE [18]. Most of the experimental values for $\sigma_{\rm non}$ on $^{\rm nat}$Pb in Fig. 1 were taken over from Fig. 28 of Ref. [5]. In addition, $\sigma_{\rm non}$ values at low neutron energies were derived from the $(n,x\gamma)$ measurements of Chapman and Morgan [19].

Among the global potentials, only that of Rapaport,

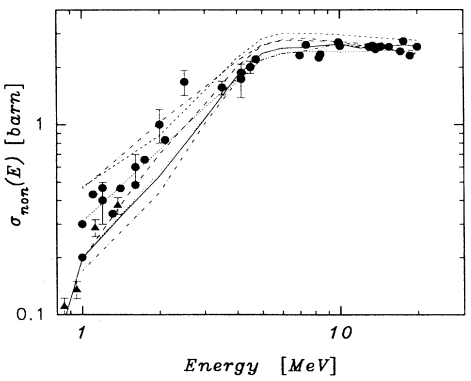


FIG. 1. The nonelastic cross section for neutrons on $^{\rm nat}$Pb. The circles represent the experimental data taken from Fig. 28 of Ref. [5], the triangles the additional data derived from an $(n,x\gamma)$ measurement [19]. The calculations were performed with the optical potentials of Becchetti and Greenlees [10] (medium-dashed line), Wilmore and Hodgson [12] (dash-dotted line), Engelbrecht and Fiedeldey [13] (short-dashed line), Rapaport, Kulkarni, and Finlay [14] (dotted line), Lawson, Guenther, and Smith [15] (dash–double-dotted line), Finlay *et al.* [16] (solid line) and Mahaux and Sartor [17] (long-dashed line).

Kulkarni, and Finlay [14] shows an appropriate agreement with measured values of the neutron total and the nonelastic cross section for $^{208}$Pb and $^{nat}$Pb. On the other hand, the potentials of Lawson, Guenther, and Smith [15], of Finlay *et al.* [16], and of Mahaux and Sartor [17] are in very good agreement with these data. Among these four nearly equally suited potentials that of Finlay *et al.* [16] was chosen. In concordance with the authors' finding, a surface real term as suggested by Ahmad and Haider [20] was included, applying a factor of 0.24.

The continuum level-density function $\rho(E, I, P)$ is factorized in GNASH as follows:

$$\rho(E, I, P) = F_P(P) F_I(I, E) \rho(E) \ , \tag{5}$$

with the parity component $F_P(P) = \frac{1}{2}$ and the spin component

$$F_I(I, E) = \frac{2I+1}{2\sigma^2(E)} \exp\left(\frac{-(I+\frac{1}{2})^2}{2\sigma^2(E)}\right) \ , \tag{6}$$

where the spin cutoff function is given by $\sigma^2(E) = C_{SC} A^{2/3} \sqrt{aE}$. $C_{SC}$ means a constant, given by either the Reffo and Herman [21] or the Gilbert-Cameron [22] prescription, and $a$ is the level-density parameter.

Three built-in models for the energy-dependent level density $\rho(E)$ are available in the GNASH code. The Gilbert-Cameron model [22] uses a constant-temperature part followed at higher excitation energies by a Fermi-gas description. The parameters of this model are the nuclear temperature $T$ and a shift parameter $E_0$ and the level-density parameter $a$, respectively. These parameters and the matching energy $E_m$ between these two descriptions are determined as described in Ref. [22].

The Ignatyuk, Smirenkin, and Tishin model [23] utilizes an energy-dependent level-density parameter $a$, otherwise it is analogous to the Gilbert-Cameron model. Beside the original Ignatyuk parametrization of the asymptotic value $\alpha$ of the level-density parameter, Arthur's parametrization [24] leading to lower level densities than using the former, was also investigated.

In addition to the above mentioned forms, it is also possible to use the backshifted Fermi-gas model [25] in GNASH.

In order to achieve a realistic description of the preequilibrium contribution, a parameter $F2$ had to be adopted for a special optical potential. It accounts for the interaction between a specific initial and final particle-hole state and thus influences the preequilibrium strength. For determining this constant $F2$, a reaction was chosen that shows a dominant preequilibrium part at the high-energy end of the spectrum, which makes the exact knowledge of the level density of the residual nucleus less crucial. A suitable reaction in this mass region is the inelastic scattering of neutrons on natural lead at an incident energy of 14.1 MeV.

Using different optical potentials and level-density models, and varying $F2$ accordingly, the neutron-production spectrum was calculated and compared with the evaluation of Pavlik and Vonach [26]. In this step, we first checked and investigated the relationship of optical potentials and level-density formulations. It turned out that not all the optical potentials were compatible with the level-density formulations used.

Using the built-in conventional Gilbert-Cameron formulation [22] with a relatively low level-density parameter $a$, one needs higher transmission coefficients produced only with the Becchetti and Greenlees [10] potential, whereas for the other potentials no good agreement with the evaluated data could be obtained. Also, the backshifted Fermi-gas model [25] seems to deliver too low values of the level density for the nuclei considered here.

It has been indicated by several authors that the energy dependence of the level density near closed shells follows a constant-temperature rather than a Fermi-gas form. In fact, a good reproduction of the neutron-production spectrum of lead is obtained using the Ignatyuk formulation as parametrized by Ignatyuk, Smirenkin, and Tishin [23] as well as by Young *et al.* [24]. The shell- and energy-dependent level-density parameter $a$ reaches essentially higher values as in the conventional Gilbert-Cameron formulation; therefore one obtains considerably higher level densities with a shape that is close to a constant-temperature form. Using the potentials of Wilmore and Hodgson [12] and of Engelbrecht and Fiedeldey [13], the best agreement is obtained with the parametrization of Arthur. The original version of Ignatyuk with still higher level densities requires lower transmission coefficients given only by the potentials of Lawson, Guenther, and Smith [15], Rapaport, Kulkarni, and Finlay [14], of Finlay *et al.* [16], and of Mahaux and Sartor [17]. For both these combinations, a value of $F2 = 2.0$ MeV$^3$ appeared appropriate.

## V. CHOICE OF PARAMETERS, RESULTS, AND DISCUSSION

As pointed out in Sec. II, it is necessary to obtain a good fit to the measured spectra already with the level densities assumed in the calculations, as only small corrections by means of Eq. (4) are permitted. Therefore a number of approaches were tried until this goal was achieved. For the reasons mentioned above, in fitting the measured neutron spectra of the proton-induced reactions, only the Ignatyuk formulation was taken into consideration with the two different parametrizations for the asymptotic value of the level-density parameter $a$. The parameters of the constant-temperature parts of the level-density formulas can be determined in a GNASH internal procedure, namely an adjustment to the number $N(E) = \int^E \rho(E')dE'$ of known discrete levels [27] at two different energies $E_l$ and $E_c$, or they can be chosen externally. Using the automated internal procedure and the asymptotic value of $a$ according to Arthur, obviously too low level densities are derived as indicated by the overestimated differential cross section in the discrete-level region, in contrast to spectra derived with the original Ignatyuk values.

Indeed, in this internal procedure, the matching of the Fermi-gas and the constant-temperature part and their derivatives comes at the price that only the difference

$N(E_c)-N(E_l)$ but not the energy dependence of $N(E)$ is reproduced. Better fits to the measured neutron-emission spectra are obtained using a mere constant-temperature formulation over the whole energy region with parameters $T$ and $E_0$ chosen to fit the cumulative number of discrete levels, taking also into consideration the energy dependence of $N(E)$ in contrast to the conventional Gilbert-Cameron method. Therefore we eventually used this functional form of the nuclear level density over the entire energy range of the analysis with the above $T$ and $E_0$ adjusted in each case for optimum fit to the experimental spectra.

For the targets $^{207,208}$Pb and $^{209}$Bi, this was first done for the lower incident energy where preequilibrium contributions are negligible. Then the spectra were calculated with the same parameters for the higher incident energy.

Difficulties were encountered in determining $T$ and $E_0$ of $^{206}$Bi owing to the shape of the density of experimentally known discrete levels. Depending on the upper end of the excitation-energy range where experimental level data are used ($E_c$), the level-density parameters and therefore the level density itself change in the manner that the lower $E_c$ is set the higher the extracted level-density results. Whereas the reproduction of density and cumulative number of known discrete levels demands an increased shift $E_0$, this results in a poorer fit of the spectrum in the discrete-level region. The presented level density is, therefore, a compromise of the spectrum-fitting procedure and of the experimentally known levels. This problem was of no importance for the other nuclei.

The best-fit spectra for all nuclides considered at the available incident proton energies are shown in Figs. 2 and 3. In these graphs, we compare the experimental neutron-emission cross sections with the calculated ones folded with the experimental energy resolution (see Sec. III). For those nuclei for which neutron spectra exist at two proton energies, the main emphasis in reproducing the spectral region of discrete levels was put on the lower incident energy. The calculated cross sections for populating the discrete-level region from the ground state up to $E_c$ agree with the experimental values within 1% for $^{207,208}$Bi and $^{209}$Po for the lower incident energy as well as for $^{204}$Bi for 11.2 MeV incident energy. On the other hand, the corresponding cross section is overestimated by 15% for $^{206}$Bi.

The resulting temperatures $T$, shifts $E_0$, and continuum edges $E_c$, together with the numbers $N(E_c)$ of discrete levels considered are presented in Table I. As shown, all nuclei demand nearly the same value of the temperature but $^{204}$Bi, for which a significantly lower temperature was obtained. Similar values of $T$ have already been found by Grimes *et al.* [28] for nuclei around $A = 200$. The second parameter $E_0$ lies lower for $^{206}$Bi than for the other residual nuclei for the reasons discussed above, and higher for $^{209}$Po due to its few levels at low excitation energies. For comparison, the table also contains the temperatures, shifts, and matching energies resulting from usage of the level-density parametrizations mentioned above in the GNASH internal matching procedure, and those from the original Gilbert-Cameron paper [22]. As apparent from the table, there is on average reasonable agreement with the temperatures from the Ignatyuk model with its original parameters, whereas the temperatures obtained with the Arthur parametrization of the Ignatyuk model seem to be systematically too high by about 15%. For the individual nuclei, however, both parametrizations yield deviations up to 30% from the temperatures derived in this work. The two parametrizations of the Gilbert-Cameron model differ with respect to the discrete levels used. The original Gilbert-Cameron parameters [22] are based on the discrete-level information of 1965, whereas the built-in version uses our present knowledge of nuclear level schemes. For this reason, the original Gilbert-Cameron parametrization in general predicts too low level densities at small excitation energies because many of the level schemes used turned out to be incomplete compared to the status used in the built-in parameter determination. At high energy, however, both versions use identical Fermi-gas parameters. Therefore the built-in matching procedure with Gilbert-Cameron

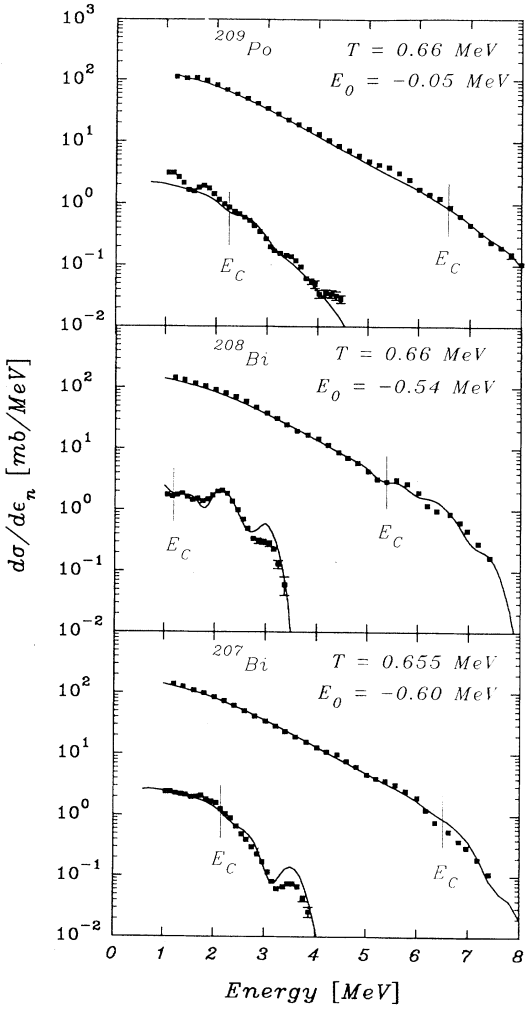


FIG. 2. Neutron-production spectra for $^{209}$Bi$(p,n)$ and for $^{207,208}$Pb$(p,n)$ at 6.95 and 11.2 MeV incident proton energy. The squares indicate the experimental data by Zhuravlev *et al.* [3,4], the lines represent the calculated values.

TABLE I. Continuum edges $E_c$ and numbers $N(E_c)$ of discrete levels considered, together with the temperatures $T$ and shifts $E_0$ resulting from the present analysis for the nuclei $^{204,206,207,208}$Bi and $^{209}$Po. For comparison, also values of $T$, $E_0$ and $E_m$ (matching energy) resulting from global level-density parametrizations are given; GC, Gilbert-Cameron.

| | Nuclide | $^{208}$Bi | $^{207}$Bi | $^{206}$Bi | $^{204}$Bi | $^{209}$Po |
|---|---|---|---|---|---|---|
| | $E_c$ (MeV) | 1.94 | 1.37 | 0.55 | 1.1 | 1.78 |
| | $N(E_c)$ | 41 | 13 | 11 | 16 | 12 |
| Best fit | $T$ (MeV) | 0.66 | 0.66 | 0.67 | 0.58 | 0.66 |
| to data | $E_0$ (MeV) | −0.54 | −0.60 | −1.15 | −0.53 | −0.05 |
| Built-in | $T$ (MeV) | 0.78 | 0.71 | 0.63 | 0.44 | 0.61 |
| orig. Ign. | $E_0$ (MeV) | −1.02 | −0.68 | −1.10 | −0.07 | 0.24 |
| | $E_m$ (MeV) | 4.58 | 4.96 | 4.93 | 2.70 | 3.92 |
| Built-in | $T$ (MeV) | 0.92 | 0.84 | 0.74 | 0.54 | 0.74 |
| Arthur | $E_0$ (MeV) | −1.63 | −1.14 | −1.47 | −0.37 | −0.16 |
| | $E_m$ (MeV) | 5.98 | 6.08 | 5.84 | 3.49 | 4.96 |
| Built-in | $T$ (MeV) | 1.05 | 0.90 | 0.86 | 0.59 | 0.69 |
| GC | $E_0$ (MeV) | −2.19 | −1.38 | −1.86 | −0.52 | −0.01 |
| | $E_m$ (MeV) | 7.22 | 6.64 | 6.80 | 3.89 | 4.58 |
| Orig. GC | $T$ (MeV) | 0.83 | 0.71 | 0.62 | | |
| [18] | $E_0$ (MeV) | −0.82 | −0.22 | −0.59 | | |
| | $E_m$ (MeV) | 3.8 | 3.7 | 2.8 | | |

Fermi-gas parameters in general results in higher nuclear temperatures and larger matching energies than the original parametrization, as can be seen from Table I. Both versions do not agree very well with the results of our analysis, as they predict either too high nuclear temperatures or too low matching energies $E_m$ to the Fermi-gas shape.

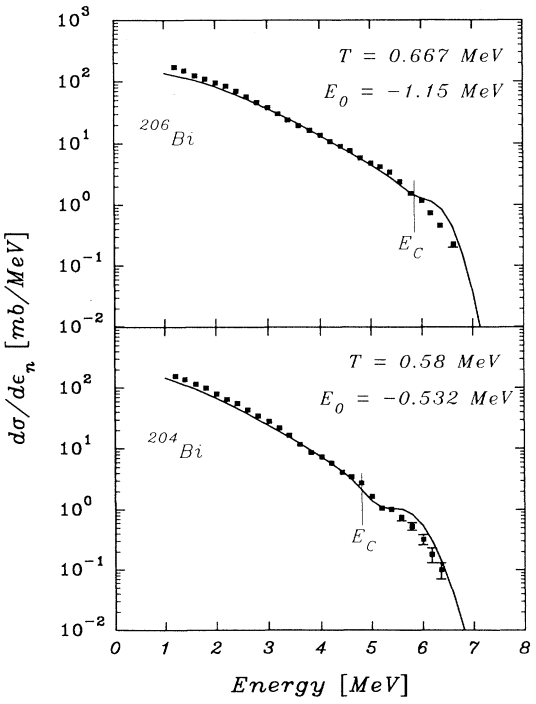


FIG. 3. Same as Fig. 2 for $^{204,206}$Pb$(p,n)$ at 11.2 MeV incident proton energy.

Finally, the constant-temperature level densities were renormalized according to Eq. (4) to account for the deviations of measured and calculated differential cross sections in the continuum region. The resulting values are displayed as solid symbols in Figs. 4 and 5.

The uncertainties of the level densities were derived in the following way. As has been pointed out by Vonach [2], rewriting Eq. (4) by multiplication with the factor $\sigma_{\text{Lev calc}}/\sigma_{\text{Lev meas}}$ which is unity as the parameters are well adjusted to reproduce $\sigma_{\text{Lev meas}}$, demonstrates that the level density is essentially determined as a quotient of two ratios, each of which is more accurate than its constituents due to the cancellation of uncertainties:

$$\rho_b(E,I,P) = \rho_b(E,I,P)|_{\text{assumed}} \frac{(d\sigma/d\varepsilon_b)/\sigma_{\text{Lev}}\big|_{\text{meas}}}{(d\sigma/d\varepsilon_b)\sigma_{\text{Lev}}\big|_{\text{calc}}} . \tag{7}$$

The various components of the uncertainty of the level density derived from the 11.2-MeV data are tabulated in detail in Table II for $^{207}$Bi as a typical example. Major contributions to the uncertainty of $[(d\sigma/d\varepsilon)/\sigma_{\text{Lev}}]_{\text{meas}}$, the measured cross-section ratio between a continuum bin and the region of discrete levels, are the following.

(a) The experimental uncertainty of the cross sections themselves which amounts to 5–13% depending on the nucleus and the excitation energy considered.

(b) The uncertainty $\Delta E_n$ in the experimental energy scale for the neutron energy which produces an uncertainty in $\sigma_{\text{Lev}}$, as the limit for integrating the cross section over the range of discrete levels may be incorrect by this amount. From the experimental conditions, $\Delta E_n$ is

TABLE II. Uncertainty contributions (in percent) to the level density of $^{207}$Bi extracted from the 11.2-MeV data (expt, experimental).

| Origin | Energy (MeV) | | | |
|---|---|---|---|---|
| | 2 | 3 | 4 | 5 |
| $\left[\frac{d\sigma}{d\varepsilon}/\sigma_{\rm Lev}\right]_{\rm meas}$, expt cross-section uncertainty | 12 | 8 | 7 | 5 |
| $\left[\frac{d\sigma}{d\varepsilon}/\sigma_{\rm Lev}\right]_{\rm meas}$, $\Delta E_n$ | 10 | 6 | 6 | 6 |
| $\left[\frac{d\sigma}{d\varepsilon}/\sigma_{\rm Lev}\right]_{\rm calc}$, spin cutoff factor | 8 | 8 | 10 | 12 |
| $\left[\frac{d\sigma}{d\varepsilon}/\sigma_{\rm Lev}\right]_{\rm calc}$, neutron transm. coeff. | 3 | 14 | 12 | 3 |
| $\left[\frac{d\sigma}{d\varepsilon}/\sigma_{\rm Lev}\right]_{\rm calc}$, preequilibrium | 26 | 13 | 5 | 5 |
| Total | 32 | 23 | 19 | 15 |

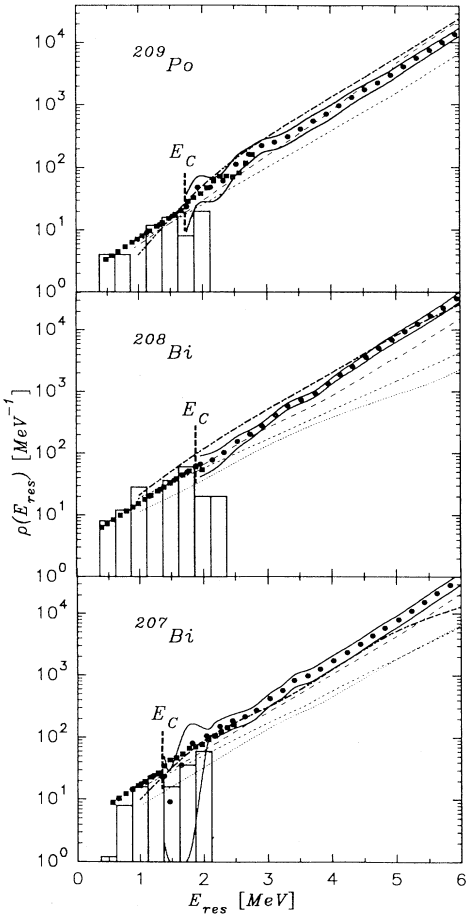


FIG. 4. Level densities for $^{209}$Po and $^{207,208}$Bi. The symbols represent the results of the present work (squares, 6.95 MeV, circles, 11.2 MeV, with solid lines indicating the range of uncertainty of the 11.2-MeV results. The histogram displays the density of low-lying levels [27], the dash–double-dotted line the results of the analysis by Zhuravlev *et al.* [3,4], the long- and short-dashed lines are Ignatyuk level density with $a$ parameter according to Ignatyuk, Smirenkin, and Tishin [23] and Young *et al.* [24], respectively, and the dotted line the Gilbert-Cameron [22] level density.

about 0.1 MeV which results in uncertainties of $\sigma_{\rm Lev}$ of 3–15 %.

The uncertainty due to preequilibrium effects is rather low (5–7 %) at excitation energies where the level-density results come from the 11.2-MeV measurement only. For those nuclei for which preequilibrium plays an important role in the discrete-level region and the first few continuum bins at the higher incoming-proton energy and hence introduces a larger uncertainty in the results, the level densities were primarily determined from the data at the additional lower incident energy of 6.95 MeV and just checked and extended by means of the 11.2-MeV data. The uncertainty in $[(d\sigma/d\varepsilon)/\sigma_{\rm Lev}]_{\rm calc}$ due to that of the spin distribution of the levels was judged by varying the spin cutoff factor. Two recommended values of the factor $C_{\rm SC}$ in Eq. (6) are those of Gilbert and Cameron [22] (0.0888) and of Reffo and Herman [21] (0.146). The level-density analyses were carried out using the mean value of 0.12 and for the uncertainty estimation repeated with

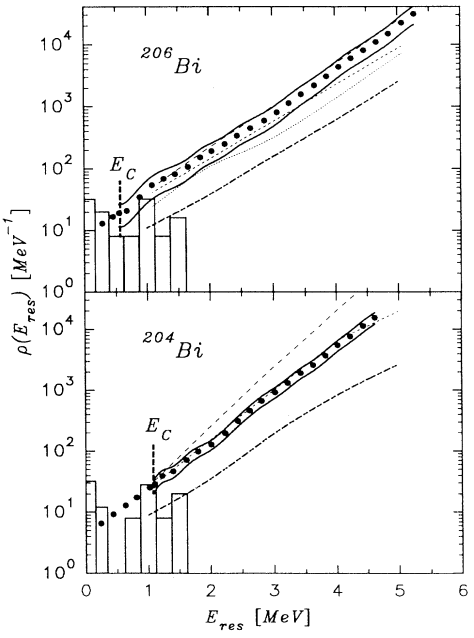


FIG. 5. Same as Fig. 4 for $^{204,206}$Bi.

the Gilbert-Cameron and the Reffo-Herman values. The deviations lie between a few percent and about 13% maximum. An important contribution to the uncertainty of $[(d\sigma/d\varepsilon)/\sigma_{\mathrm{Lev}}]_{\mathrm{calc}}$ comes from the inaccurate knowledge of the transmission coefficients. The statistical calculations were, therefore, repeated using another optical potential. Among the more recent potentials [14–17] investigated in Sec. IV, that of Mahaux and Sartor [17] shows the largest deviation in $\sigma_{\mathrm{non}}$ from the Finlay *et al.* potential [16] used for the analysis. With the potential of Mahaux and Sartor [17], the derived level densities are higher than with that of Finlay *et al.* [16], but cross over at excitation energies of several MeV.

An additional uncertainty is introduced by the choice of the energy $E_c$ up to which the discrete-level scheme is used, as the judgment up to which energy all levels and their correct spins and parities are known is somewhat subjective. This uncertainty was determined by estimating reasonable upper and lower limits for $E_c$ and repeating the calculation of the level densities with these $E_c$ values. The effect was largest for $^{206}$Bi for which it introduced an uncertainty of $\approx 25\%$.

The total uncertainties at four different excitation energies are compiled for all considered nuclei for 11.2 MeV incident proton energy in Table III. These values define the lower and upper boundary of the bands of uncertainty drawn in Figs. 4 and 5. For reasons of clarity, for the 6.95-MeV results no uncertainties are displayed in Fig. 4. They are smaller than at 11.2 MeV due to the lacking preequilibrium component and amount to 15–20 %. Within the given uncertainties, there is complete agreement between the results derived from the measurements at the two incident energies.

As can be seen from Figs. 4 and 5, our results are satisfactorily compatible with those of Zhuravlev *et al.* [3] and Biryukov *et al.* [4] for the nuclei $^{209}$Po and $^{207,208}$Bi, if we assume that the uncertainties in Zhuravlev *et al.*'s analysis are about equal to ours. For $^{204,206}$Bi, the level densities derived in Ref. [3] deviate strongly from our results. This is most probably due to an incorrect estimate of the number of discrete levels in Ref. [3]. Using the level schemes of the rather old *Table of Isotopes* [29], they assumed a total number of three levels in the energy range 0–1 MeV, whereas according to Ref. [27] there are now 12 levels known in this excitation-energy range. For this reason, the level densities of Ref. [3] for $^{204,206}$Bi should be multiplied by a factor of approximately 4, which would bring them in satisfactory agreement with our results.

The extracted level densities were also compared with the Ignatyuk model, using the GNASH internal procedure for determining $T$ and $E_0$, and for the asymptotic $a$ value

TABLE III. Total uncertainty (in percent) of the level densities of $^{204,206,207,208}$Bi and $^{209}$Po extracted from the 11.2-MeV data, given for different excitation energies.

| Nuclide | Energy (MeV) | | | |
|---|---|---|---|---|
| | 2 | 3 | 4 | 5 |
| $^{208}$Bi | 37 | 13 | 11 | 16 |
| $^{207}$Bi | 32 | 23 | 19 | 15 |
| $^{206}$Bi | 35 | 35 | 31 | 32 |
| $^{204}$Bi | 18 | 20 | 20 | 22 |
| $^{209}$Po | 47 | 23 | 25 | 19 |

the Ignatyuk and the Arthur parameters, respectively, and with the predictions of the Gilbert-Cameron model [22]. The level densities computed with the Ignatyuk parameters agree with our extracted values for $^{206,207}$Bi and $^{209}$Po very well, and only slightly less well for $^{208}$Bi. Arthur's parameters yield smaller slopes of the level densities. Compared to the Ignatyuk parametrization, this improves the agreement with our results in the case of $^{204}$Bi and makes it worse for $^{206,207,208}$Bi and $^{209}$Po.

## VI. SUMMARY

The goal of the present investigation was the extraction of level densities by way of a reanalysis of the neutron-production spectra from $(p,n)$ reactions on $^{204,206,207,208}$Pb and $^{209}$Bi measured by Zhuravlev *et al.* [3,4], with particular interest in the consistency between the respective results and the question of error estimate, as well as the quality of the description of the resulting level densities by means of global parametrizations of commonly used level-density formulations. Absolute values for the level densities of the investigated nuclei could be derived with uncertainties of 15–35 %. We found that there is fair agreement in the results of the two analyses for some of the nuclei, whereas there is quite some discrepancy for other nuclides. It appears that the degree of consistency depends on whether or not the neutron-production spectrum existed at just the higher (11.2 MeV) or also the lower (6.95 MeV) incident proton energy, and on the quality of reproduction of the spectrum in the energy range where discrete levels are populated.

As far as the comparison of the extracted level densities with those calculated from standard formulae with global parameters goes, there is agreement within a factor of 4, at most.

[1] M. K. Mehta, IAEA, Vienna, Report No. INDC/P (83)-41, 1983.

[2] H. Vonach, Proceedings of the IAEA Advisory Group Meeting on Basic and Applied Problems of Nuclear Level Densities, Upton, New York, 1983, Brookhaven National Laboratory Report No. BNL-NCS-51694, 1983, p. 247.

[3] B. V. Zhuravlev, N. N. Titarenko, and V. I. Trykova, FEI report, Institute of Physics and Power Engineering, Obninsk, 1988; B. V. Zhuravlev, N. S. Biryukov, A. P. Rudenko, N. N. Titarenko, and V. I. Trykova, IAEA, Vienna, Report No. INDC(NDS)-234,1990, p. 91.

[4] N. S. Biryukov, B. V. Zhuravlev, A. P. Rudenko, and V.

I. Trykova, in Proceedings of the 36th All Union Conference on Nuclear Spectroscopy and Nuclear Structure, Kharkov, Ukraine, 1986, p. 307.
[5] P. G. Young and E. D. Arthur, Los Alamos National Laboratory, Report No. LA-6947, 1977; P. G. Young, E. D. Arthur, and M. B. Chadwick, Los Alamos National Laboratory, Report No. LA-UR-92-205, 1992.
[6] O. Bersillon, Progress Report of the Nuclear Physics Division, Bruyères-le-Châtel 1977, Report No. CEA-N-2037, 1978, p. 111; O. Bersillon, in *Proceedings of the Workshop on Applied Nuclear Theory and Nuclear Model Calculations for Nuclear Technology Applications*, Trieste, Italy, 1988, edited by M. K. Mehta and J. J. Schmidt (World Scientific, Singapore, 1989), p. 319.
[7] F. G. Perey, Phys. Rev. **131**, 745 (1963).
[8] T. Mo and R. H. Davis, Phys. Rev. C **6**, 231 (1972).
[9] G. S. Mani, M. A. Melkanoff, and I. Iori, Saclay Report No. CEA-2379, 1963.
[10] F. D. Becchetti, Jr., and G. W. Greenlees, Phys. Rev. **182**, 1190 (1969).
[11] C. Mahaux and R. Sartor, Nucl. Phys. **A503**, 525 (1989).
[12] D. Wilmore and P. E. Hodgson, Nucl. Phys. **55**, 673 (1964).
[13] C. A. Engelbrecht and H. Fiedeldey, Ann. Phys. (N.Y.) **42**, 262 (1967).
[14] J. Rapaport, V. Kulkarni, and R. W. Finlay, Nucl. Phys. **A330**, 15 (1979).
[15] R. D. Lawson, P. T. Guenther, and A. B. Smith, Phys. Rev. C **36**, 1298 (1987); see also Ref. [1] in Nucl. Phys. **A493**, 267(E) (1989).
[16] R. W. Finlay, J. R. M. Annand, T. S. Cheema, J. Rapaport, and F. S. Dietrich, Phys. Rev. C **30**, 796 (1984).
[17] C. Mahaux and R. Sartor, Nucl. Phys. **A516**, 285 (1990).
[18] M. Uhl and B. Strohmaier, Institut für Radiumforschung and Kernphysik, Vienna, Report No. IRK 76/01, 1976, and Addenda to this report.
[19] G. T. Chapman and G. L. Morgan, Oak Ridge National Laboratory Report No. ORNL-TM-4822, 1975.
[20] I. Ahmad and W. Haider, J. Phys. G **2**, 157 (1976).
[21] G. Reffo and M. Herman, Lett. Nuovo Cimento **34**, 261 (1982).
[22] A. Gilbert and A. G. W. Cameron, Can. J. Phys. **43**, 1248 (1965).
[23] A. V. Ignatyuk, G. N. Smirenkin, and A. S. Tishin, Sov. J. Nucl. Phys. **21**, 255 (1975).
[24] P. G. Young, E. D. Arthur, M. Bozoian, T. R. England, G. M. Hale, R. J. LaBauve, R. C. Little, R. E. MacFarlane, D. G. Madland, R. T. Perry, and W. B. Wilson, Trans. Am. Nucl. Soc. **60**, 271 (1989); Los Alamos National Laboratory Report No. LA-11753-MS, 1990.
[25] W. Dilg, W. Schantl, H. Vonach, and M. Uhl, Nucl. Phys. **A217**, 269 (1973).
[26] A. Pavlik and H. Vonach, Phys. Data **13**-4 (1988).
[27] M. R. Schmorak, Nucl. Data Sheets **43**, 383 (1984); M. J. Martin, *ibid.* **47**, 797 (1986); M. R. Schmorak, *ibid.* **50**, 719 (1987); R. A. Helmet and M. A. Lee, *ibid.* **61**, 93 (1990); M. J. Martin, *ibid.* **63**, 723 (1991).
[28] S. M. Grimes, J. D. Anderson, J. W. McClure, B. A. Pohl, and C. Wong, Phys. Rev. C **6**, 236 (1972).
[29] *Table of Isotopes*, edited by C. M. Lederer and V. S. Shirley, 7th ed. (Wiley Interscience, New York, 1978).